ChemComm

Accepted Manuscript

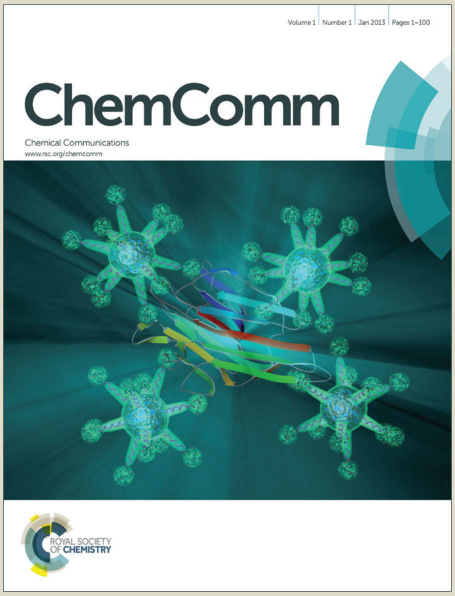

ROYAL SOCIETY OF **CHEMISTRY**

www.rsc.org/chemcomm

Journal Name RSCPublishing

COMMUNICATIONS

Cite this: DOI: 10.1039/x0xx00000x

A new class of electrocatalyst of supporting Pt on an Engel-Brewer alloy substrate: A demonstration for oxidation of ethylene glycol

Received 00th January 2012,
Accepted 00th January 2012

DOI: 10.1039/x0xx00000x

X.F. Yang,[a] W. Xu,[a] M. Li,[a] B. E. Koel,*[b] and J.G. Chen*[c]

A novel electrocatalytic surface consisting of a Pt monolayer (ML) on an Hf-Ir alloy substrate demonstrated significantly higher activity (six times) and higher selectivity to CO_2 formation than bulk Pt in oxidizing ethylene glycol. This enhanced performance could be associated with the high reducibility of Hf oxide and altered electronic property of the Pt ML.

Hydrogen gas (H_2) is currently the primary fuel used in low temperature fuel cells because of its facile oxidation at the anode. However, difficulties in transportation and storage of H_2 gas are often cited as impediments to broad utilization. The high volume energy density and simplicity in handling of some simple alcohols and polyols, such as methanol, ethanol, and ethylene glycol (EG), have prompted their potential use as alternative to H_2 gas.[1,2] EG stands out to have some unique advantages.[3] For instance, the existing infrastructure is well developed for production of EG as it has been used as the major coolant by auto industry. EG is also less toxic than methanol, and more importantly it could be produced directly from non-food based biomass such as cellulose and hemicellulose.[4]

However, it is quite challenging to fully oxidize EG into CO_2 because of large activation energies or over-potentials for breaking the carbon-carbon bond. [5,6] Partial oxidation of EG catalyzed by Pt mainly produces undesired glycolate and oxalate species, which lowers the output voltage and results in low Faraday efficiency.[7-9] Therefore, it is important to develop high performance catalysts to enhance the overall oxidation activity and the selectivity to CO_2.[10-12] Here, we report a new class of active electrocatalyst consisting of Pt on an Engel-Brewer alloy, which is a class of compounds from the alloying of early and late transition metals. Specifically, Pt ML on the Hf-Ir alloy substrate (Pt ML/Hf-Ir) is compared with pure Pt and ML Pt on a precious metal substrate (Ir). The electronic structure of surface Pt is modified by the lattice mismatch between the Pt adlayer and the Hf-Ir alloy substrate, while the highly reducible Hf oxide supplies active oxygen atoms to assist the C-C bond scission. This study has demonstrated that the combination of active Pt and reducible Hf oxide provides exceptional oxidation capability in oxidizing EG to CO_2. Furthermore, as a typical Engel-Brewer compound, the Hf-Ir alloy is characterized by its physical strength and chemical stability. These properties are highly desired for stable electrocatalysts which work in strong acidic or alkaline environments.

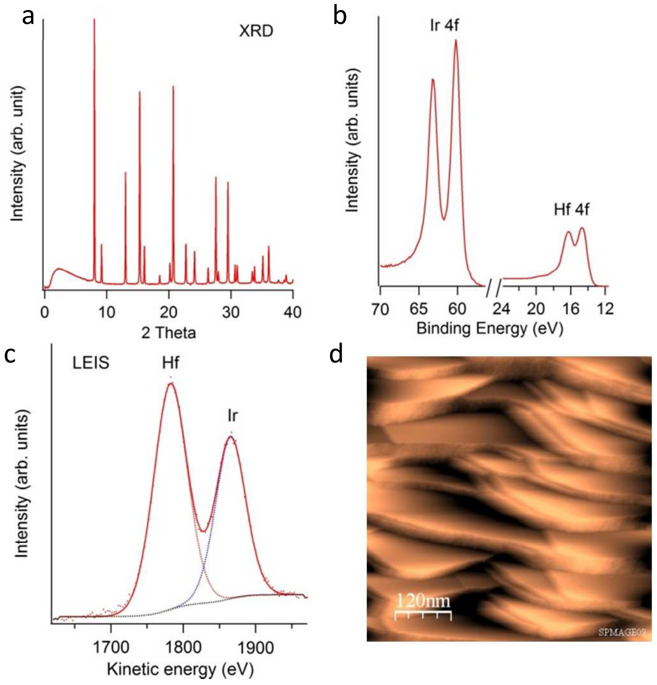

Fig. 1 Surface characterization of the Hf-Ir alloy substrate. (a) Glancing-incidence XRD pattern for Hf-Ir polycrystalline bulk alloy. X-ray source: synchrotron radiation, 0.3196 Å. (b) XPS spectra of the clean Hf-Ir alloy in the Ir 4f and Hf 4f regions. (c) LEIS spectrum of the clean Hf-Ir alloy. (d) An STM image of the Hf-Ir alloy surface (600×600 nm^2).

A clean Hf-Ir polycrystalline sample was prepared by Ar+ sputtering and vacuum annealing in an ultrahigh (UHV) chamber equipped with surface characterization techniques including X-ray photoemission spectroscopy (XPS), low energy ion scattering (LEIS) and scanning tunneling microscopy (STM) to examine surface composition and structure. The crystal structure of the Hf-Ir alloy was also examined by X-ray diffraction (XRD). Fig. 1a shows the XRD pattern of the Hf-Ir alloy with glancing-incident X-ray beam. It matches the standard XRD pattern of a face centered cubic (FCC) structure with the measured lattice constant of 397 pm. The expansion suggests that the Hf atoms adopt the FCC structure of Ir and cause the Ir lattice (384 pm) to expand by 3.3%. Fig. 1b shows the XPS spectra of the cleaned Hf-Ir alloy in the Hf 4f and Ir 4f regions. The binding energy (BE) of the Ir $4f_{7/2}$ peak was found at 60.6 eV, which is 0.7 eV lower than that of a pure Ir sample (61.3 eV), indicating strong alloying interaction between Hf and Ir. The topmost layer surface composition was probed by LEIS, as shown in Fig. 1c. LEIS revealed a surface composition of Ir:Hf of 2:3, significantly different from the bulk ratio, 3:1. Fig. 1d shows a typical surface structure of a clean Hf-Ir alloy. Large atomic flat (111) terraces (50-100 nm) and multiple steps are present at the surface. The preference to form (111) terraces can be understood by the fact that (111) plane has the lowest free energy in the FCC structure. After the preparation of the clean Hf-Ir surface, a single monolayer of Pt was deposited at the surface by physical vapor deposition (PVD) using a Pt evaporator. As a comparison a monolayer of Pt was deposited on a clean polycrystalline Ir sample. A clean polycrystalline Pt sample was also prepared in UHV. Details related to preparation and determination of a Pt ML can be found in Supporting Information.

To investigate the electrocatalytic activity for EG oxidation, both cyclic voltammetry (CV) and chronoamperometry (CA measurements were performed in alkaline conditions. Fig. 2a shows typical stable CV curves of electrocatalytic oxidation of 0.2 M EG in 0.1 M KOH solution at a linear scan rate of 50 mV/s. The onset for the EG oxidation current for bulk Pt appeared at 420 mV, reached a maximum at 950 mV, and then rapidly decreased. The ethylene glycol oxidation reaction (EGOR) CV curves on the Pt ML surfaces were very different and no peak features developed in this potential range. The decrease of oxidation current at high potentials is often caused by surface oxidation or poisoning effect of strongly adsorbed OH^-. In the supporting information, CVs of these three surfaces without EG are compared in Fig. S2. It clearly shows that the onset potential for surface oxidation on the Pt ML surfaces occurs at a higher potential than that on the Pt surface. Thus, the strong resistance to oxidation of the Pt ML surfaces is likely responsible for the absence of oxidation peaks below 1050 mV. The EGOR onset potentials on Pt ML/Ir and Pt ML/Hf-Ir appeared at 320 and 250 mV, respectively. The large decrease in over potential indicated that EG was oxidized with smaller reaction barrier at the Pt ML/Hf-Ir surface. CA measurements of these three surfaces under the same conditions at a fixed potential of 500 mV vs RHE are shown in Fig. 2b. The Pt ML surfaces generated 4-6 times higher current than the bulk Pt surface, demonstrating the high EGOR activity of the Pt ML surfaces.

Although the CV and CA results revealed enhanced activities of the ML Pt surfaces, these measurements did not provide information on whether EG is completely oxidized to CO_2. Thus, the reaction intermediates and products were further studied using *in-situ* IRRAS at various potentials relative to the reference spectra at 50 mV. In these *in-situ* IRRAS spectra, positive peaks are related to the appearance of new species or increasing concentrations, while negative peaks represent decreasing concentrations. The IR peak positions and the corresponding vibrational modes are summarized in Supporting Table 1. As shown in Fig. 3a, the low intensity of the broad feature near 1400 cm^{-1} at 827 mV indicates the formation of small amount of carbonates. The small peak at 2340 cm^{-1} appears at 1152 mV, corresponding to the formation of CO_2. However, the bands from glycolate and oxalates species dominate in all spectra. Thus, the main products from EG oxidation on a Pt surface are glycolate and oxalate species, generated from partial oxidation of EG without breaking the C-C bond. The IRRAS spectra from the Pt ML/Ir surface were shown in Fig. 3b with its peaks very similar to those from the Pt surface except that the intensities at 1072, 1322, and 1231 cm^{-1} are larger and the board negative OH band between 2500 and 3000 cm^{-1} reaches its maximum at lower potential (1090 mV). These results suggest that Pt ML/Ir is more active than Pt for EG oxidation, consistent with the CV and CA measurements. But the main oxidation products by Pt ML/Ir are still glycolate and oxalate.

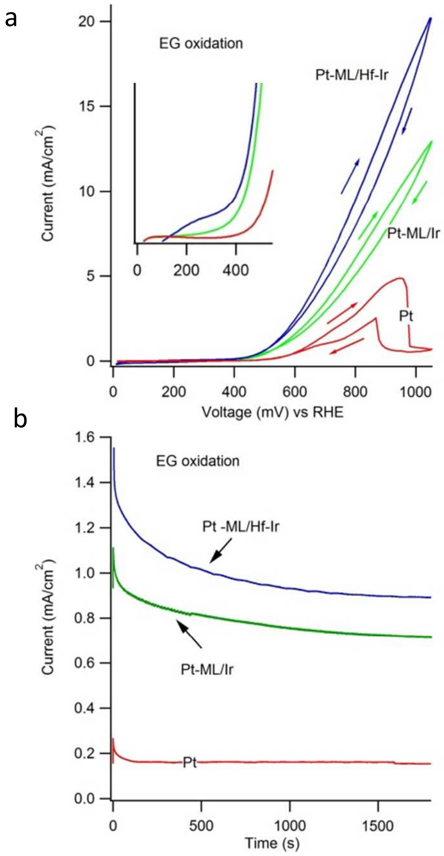

Fig. 2 Electrocatalytic oxidation of 0.2 mol/L EG in 0.1 mol/L KOH on the Pt, Pt ML/Ir and Pt ML/Hf-Ir surfaces at 25 ºC. (a) Cyclic voltammogram (CV) of 10th scan with a scan rate of 50 mV/s. Inset: zoomed view of onset regions from EG oxidation during the forward scans. (b) Chronoamperometric (CA) responses for all surfaces at 0.5 V vs RHE.

In comparison, the Pt ML/Hf-Ir surface (Fig. 3c) shows enhancement in both the overall activity and the selectivity to carbonates or CO_2, as evidenced by the more intense peaks of near 1400 and 2340 cm^{-1} and their appearance at lower potentials (Fig. S3). The OH band intensity reaches its negative maximum at the potential as low as 792 mV due to the full depletion of OH^- ion in the thin layer between the sample surface and IR window. As a consequence, the carbonates transform to CO_2, producing a negative feature at 1389 cm^{-1}.

This negative band caused by the decrease of carbonate concentration can be more obviously seen by the difference in two continuous spectra show in Supportng Fig. S4. Based on the peak intensity at 2340 cm^{-1}, the relative amount of CO_2 produced on these three surfaces are in the order of Pt ML/Hf-Ir>Pt ML/Ir ≈ Pt. Furthermore, IRRAS results suggest that complete oxidation of EG to carbonate by Pt ML/Hf-Ir surface occurs as 470 mV during CA measurement, which is shown in Supporting Fig. S5. Therefore, the comparison of these three surfaces in the IRRAS study clearly demonstrates the important role of the Hf-Ir substrate for achieving higher overall activity and higher selectivity to C-C bond cleavage to produce the fully oxidized product of carbonates/CO_2.

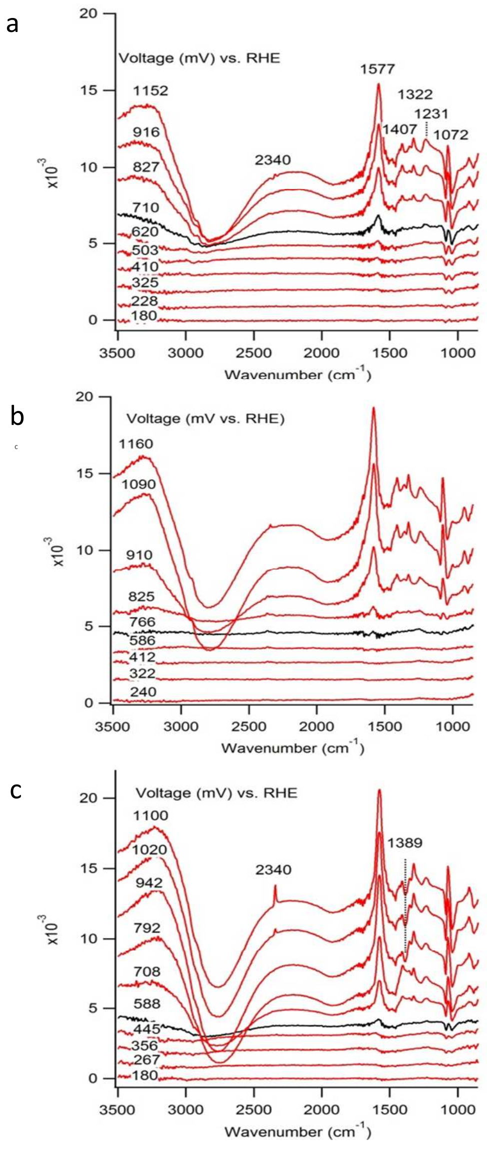

Fig. 3 *In-situ* IRRAS spectra recorded during EGOR on three surfaces. (a) Pt, (b) Pt ML/Ir and (c) Pt ML/Hf-Ir. Scan rate 1 mV/s. The spectra highlighted by black color show the beginning of producing carbonates.

Electrochemical oxidation of alcohols by H_2O has been proposed to be governed by a bi-functional process that involves oxygenate intermediates and hydroxide coadsorption on the surface, followed by the oxidation of these intermediates by hydroxides.[13,14] This mechanism explains well the promotion effect of ruthenium in Pt-Ru and tin in Pt-Sn alloy catalytic systems for ethanol oxidation, where H_2O prefers to adsorb and dissociate on Ru and Sn sites.[15,16] Similarly, foreign metal ad-atoms (Bi and Pb) on Pt surfaces are also reported to largely improve the activity for EG oxidation.[17,18] In the present study, multiple oxidation states of Hf at the surface of these samples were revealed by XPS after the sample was exposed to electrolyte. Some of surface Hf is present as partially oxidized HfO_x, $1<x<2$. HfO_x can be further oxidized to HfO_2 at low O_2 pressure and HfO_2 can be easily reduced to HfO_x by vacuum annealing at 600 K. More discussion regarding Hf-oxide reducibility is described in Supporting Fig. S6. Thus, some of the oxygen atoms in HfO_2 can be relatively easily donated for oxidizing the adsorbed oxygenate intermediates. Formation of Hf oxide alone on Pt ML/Hf is not sufficient to improve the performance of the Pt layer (Fig. S7), but it is very important to improve the selectivity to CO_2 product. As shown in the IRRAS measurements, the main products by the Pt ML/Ir surface are still from incomplete oxidation of EG and more carbonate/CO_2 is produced by the Pt ML/Hf-Ir surface with the presence of HfO_x. Another key factor strongly influencing the electrocatalytic alcohol oxidation is the binding strength of intermediates, which is largely determined by the electronic properties of Pt. It is well known that the electronic and strain effects can lead to changes in the binding energies and reaction pathways of adsorbates on the Pt (Pd) ML structures, [19-24] which also likely contribute to the high activity of the Pt ML supported on Hf-Ir.

Electrocatalytic stability is critical for maintaining long-term high performance of fuel cells. This issue becomes even more important if the electrocatalyst has a low loading of Pt, such as the case of ML Pt catalysts. The stability of Pt ML/Hf-Ir surface was investigated using XPS analysis of the Pt 4f and Hf 4f regions before and after EG oxidation (Fig. 4). XPS showed no noticeable change of the Pt/Ir peak ratio, indicating good stability of the Pt ML under these electrochemical conditions. The stability of Hf was also identified by the unchanged Hf 4f total peak intensity, even though the oxidation state of some surface Hf was altered after electrochemical measurements. However, the oxidation of Hf suggests that the Pt ML may not perfectly cover the whole surface or it may reconstruct to form clusters during reaction. As shown in supporting Fig. S6, Hf can easily change its oxidation states (Hf $^{2+}$<-> Hf $^{4+}$) upon the change of environments and this property in donating oxygen is most likely important for enhancing the activity in oxidizing surface intermediates.

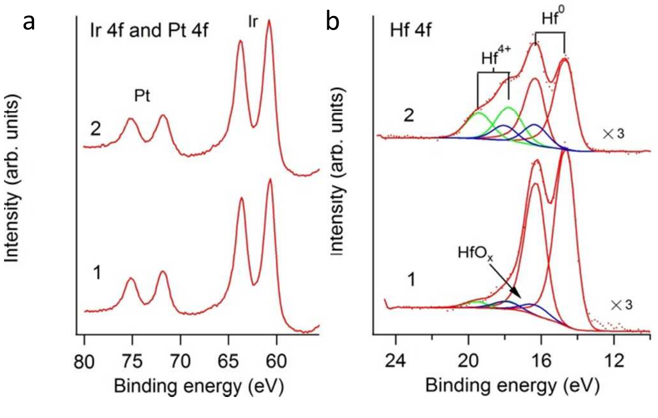

Fig. 4 XPS analysis of Pt ML/Hf-Ir before (1) and after (2) electrochemical measurements. (a) Pt 4f and Ir 4f regions. (b)

Hf 4f region. More details of XPS analysis are described in the Supplementary Information.

It should be pointed out that the loading of precious metal (Ir) in the substrate represents a potential concern for practical electrocatalysts. Ir alone does not have any apparent catalytic activity for EGOR (not shown), and the main role for Ir is to form the Hf-Ir alloy that supports and modifies the Pt monolayer. Considering that there is only 0.4 ML Ir on the surface of the Hf-Ir alloy substrate (Fig. 1c), a Hf-Ir alloy substrate with lower bulk Ir concentration should have a similar performance as the studied $HfIr_3$ alloy. Other stable Engel-Brewer compounds (alloys of early and late transitional metals) without Ir should also be explored.

In summary, electrocatalysts consisting of a Pt ML on the Hf-Ir alloy substrates were synthesized and characterized using UHV techniques and their performance was studied in an electrochemical cell by CV and CA for direct EG oxidation in alkaline conditions. The Pt ML surfaces demonstrated significantly enhanced EGOR activities (six times) over bulk Pt. *In-situ* IRRAS of Pt ML on Hf-Ir verified a much lower onset potential for EG oxidation and a higher selectivity to CO_2 formation. XPS analysis of the surface before and after electrochemical measurements confirmed good stability of the Pt-monolayer structure. This enhanced performance could be associated with the high reducibility of Hf oxide and the altered electronic property of the Pt ML. This study identifies a highly active catalysis system with an ultralow amount of Pt using EG as prospective fuel. Future studies should focus on reducing or avoiding Ir in the catalysts with other Engel-Brewer compound and further improving the selectivity to CO_2.

We acknowledge support of this work by the National Science Foundation (Grant No. CHE-1129417) and Brookhaven National Laboratory, supported by the U.S. DOE/BES, under Contract No. DE-AC02-98CH10886, LDRD Project no. 13-038. We thank Dr. Radoslav Adzic for his help on IRRAS and his comments on this work.

Notes and references

[a] Chemistry Department, Brookhaven National Laboratory, Upton, New York 11973, USA
[b]Department of Chemical and Biological Engineering, Princeton University, Princeton, NJ 08544, USA Email: bkoel@princeton.edu
[c]Department of Chemical Engineering, Columbia University, New York, NY 10027, USA Email: jgchen@columbia.edu

† Electronic Supplementary Information (ESI) available: Experimental details, Determination of Pt monolayer by XPS, Comparison of CVs of Pt, Ir and Pt ML/Hf-Ir surfaces, IRRAS spectra of EG oxidation at fixed potential, and Reducibility of HfOx. See DOI: 10.1039/c000000x/

(1) Lamy, C.; Belgsir, E. M.; Léger, J. M. *J. Appl. Electrochem.* **2001**, *31*, 799.

(2) Song, S.; Tsiakaras, P. *Appl. Catal., B* **2006**, *63*, 187.

(3) Serov, A.; Kwak, C. *Appl. Catal., B* **2010**, *97*, 1.

(4) Yue, H.; Zhao, Y.; Ma, X.; Gong, J. *Chem Soc Rev* **2012**, *41*, 4218.

(5) Matsuoka, K.; Iriyama, Y.; Abe, T.; Matsuoka, M.; Ogumi, Z. *J. Electrochem. Soc.* **2005**, *152*, A729.

(6) Cherstiouk, O. V.; Savinova, E. R.; Kozhanova, L. A.; Parmon, V. N. *React. Kinet. Catal. Lett,* **2000**, *69*, 331.

(7) Marchionni, A.; Bevilacqua, M.; Bianchini, C.; Chen, Y.-X.; Filippi, J.; Fornasiero, P.; Lavacchi, A.; Miller, H.; Wang, L.; Vizza, F. *ChemSusChem* **2013**, *6*, 518.

(8) Demarconnay, L.; Brimaud, S.; Coutanceau, C.; Léger, J. M. *J. Electroanal. Chem.* **2007**, *601*, 169.

(9) de Lima, R. B.; Paganin, V.; Iwasita, T.; Vielstich, W. *Electrochim. Acta* **2003**, *49*, 85.

(10) Bambagioni, V.; Bevilacqua, M.; Bianchini, C.; Filippi, J.; Marchionni, A.; Vizza, F.; Wang, L. Q.; Shen, P. K. *Fuel Cells* **2010**, *10*, 582.

(11) Zheng, J.-N.; Lv, J.-J.; Li, S.-S.; Xue, M.-W.; Wang, A.-J.; Feng, J.-J. *J. Mater. Chem. A* **2014**, *2*, 3445.

(12) Feng, J.-J.; Zhou, D.-L.; Xi, H.-X.; Chen, J.-R.; Wang, A.-J. *Nanoscale* **2013**, *5*, 6754.

(13) Watanabe, M.; Motoo, S. *J. Electroanal. Chem. Interfacial Electrochem.* **1975**, *60*, 267.

(14) Koper, M. T. M.; Lukkien, J. J.; Jansen, A. P. J.; van Santen, R. A. *J. Phys. Chem. B* **1999**, *103*, 5522.

(15) Li, H.; Sun, G.; Cao, L.; Jiang, L.; Xin, Q. *Electrochim. Acta* **2007**, *52*, 6622.

(16) Zhou, W. J.; Song, S. Q.; Li, W. Z.; Zhou, Z. H.; Sun, G. Q.; Xin, Q.; Douvartzides, S.; Tsiakaras, P. *J. Power Sources* **2005**, *140*, 50.

(17) Kadirgan, F.; Beden, B.; Lamy, C. *J. Electroanal. Chem. Interfacial Electrochem.* **1983**, *143*, 135.

(18) Pierre, G.; Ziade, A.; El Kordi, M. *Electrochim. Acta* **1987**, *32*, 601.

(19) Sasaki, K.; Wang, J. X.; Naohara, H.; Marinkovic, N.; More, K.; Inada, H.; Adzic, R. R. *Electrochim. Acta* **2010**, *55*, 2645.

(20) Kibler, L. A.; El-Aziz, A. M.; Hoyer, R.; Kolb, D. M. *Angew. Chem. Int. Ed.* **2005**, *44*, 2080.

(21) Hammer, B.; Morikawa, Y.; Nørskov, J. K. *Phys. Rev. Lett.* **1996**, *76*, 2141.

(22) Zhang, J.; Mo, Y.; Vukmirovic, M. B.; Klie, R.; Sasaki, K.; Adzic, R. R. *J. Phys. Chem. B* **2004**, *108*, 10955.

(23) Lima, F. H. B.; Gonzalez, E. R. *Appl. Catal., B* **2008**, *79*, 341.

(24) Zhang, J.; Vukmirovic, M. B.; Xu, Y.; Mavrikakis, M.; Adzic, R. R. *Angew. Chem. Int. Ed.* **2005**, *44*, 2132.